Representation of Spatial Orientation by the Intrinsic Dynamics of the Head-Direction Cell Ensemble: A Theory

Aekkrit Kuntipalo,[1] Chetan Mathias,[1] Santhosh Raj Srinivasan,[1] and Jonathan Undelikwo[1]

[1]*School of Psychology, University of Nottingham, Nottingham, NG7 2RD, UK*

Head direction (HD) cells are central to spatial orientation as they encode an animal's directional heading regardless of the animal's location. Using Python packages such as SciPy's `solve_ivp` and `ddeint`, we successfully replicated and extended the computational model of the HD cells proposed by Kechen Zhang in "Representation of spatial orientation by the intrinsic dynamics of the head-direction cell ensemble: a theory" *Journal of Neuroscience* 16.6 (1996): 2112-2126. Extending the work, we used delay differential equations (DDEs) to account for delays in neuronal signal transmission and spike frequency adaptation to account for the effects of neuronal fatigue. Our findings validate the original model in sustaining stable bump attractor dynamics, and the addition of DDEs adds oscillatory behaviour and delayed propagation effects that make the model more biologically realistic. Spectral analysis shows that the DDE model has more power at lower frequencies with more temporal dynamics compared to the original model. The findings strengthen the importance of time-dependent feedback among HD cell networks and give insight into how neural circuits enable spatial navigation.

I. INTRODUCTION

Navigation is a critical cognitive function that is essential for the survival of mammals. The head direction (HD) cells constitute a population of neurons that contribute significantly to spatial orientation by effectively encoding the direction of an animal's heading [1]. When animals such as rats turn their heads to look in a certain direction, the HD cells spike according to the head's orientation, irrespective of the animal's location, even in dark environments [1, 2]. HD cells are found in many regions of the brain, especially within the limbic system [3]. The key areas with a large population of HD cells include the postsubiculum, the anterior thalamic nuclei and the lateral mammary nuclei [4]. HD cells in these areas exhibit a preferred firing direction, meaning they fire maximally when the head is oriented in a specific direction [1]. Consequently, these cells give a continuous representation of direction heading that is necessary for a sense of direction and spatial orientation.

These insights into the functioning of HD cells have enabled the creation of computational models that mimic their function. Such models, provide a helping hand to understand the mechanisms underlying our sense of direction. One such model has been developed by Zhang [1]. Zhang's [1] model explains how HD cells maintain a stable representation using self-motion cues for updating and visual landmarks for calibration. The model uses attractor dynamics coupled with a dynamic shift mechanism based on synaptic weight distribution, thus allowing smooth and accurate directional tracking.

We extend Zhang's [1] model by incorporating spike frequency adaptation (SFA) to mimic neuronal fatigue and delay differential equations (DDEs) to model the temporal delays present in signal propagation. Including these characteristics allows for a more accurate representation of real neuronal behaviour, realistically mimicking slow orientation changes and oscillatory behaviour typical of biological systems.

Using mathematical modelling techniques, namely the Fast Fourier Transform (FFT), which allows for efficient calculation of synaptic interactions, we explored the stability of the HD cell network and the impact of different weight changes on the spatial representation. Our results show that delays produce more intricate temporal behaviour, as illustrated by reduced propagation of activity bumps and increased oscillatory behaviour. Additionally, we investigate the relevance of these results to artificial intelligence, specifically in the creation of biologically inspired navigation systems.

By refining Zhang's [1] HD cell model with biologically plausible mechanisms, this work provides a better understanding of the neural computation intrinsic to spatial orientation and a foundational platform for the development of neural-inspired algorithms in robotics and artificial intelligence.

II. BASIC PROPERTIES OF HD CELLS

A. General Properties

HD cells were recorded using electrodes in freely moving rats placed in enclosures with visual cue cards by Taube et. al. [5]. Initially, the rats were

placed in a cylindrical enclosure with a white cue card attached to the wall. In each trial, the cue card was rotated 90°, 180° and 270°. Additionally, the shape of the enclosure was changed to a rectangle and then a square to examine whether environmental geometry influenced HD cell activity. The results showed that the preferred firing direction of the HD cells shifted when the cue card was rotated, indicating that HD cells rely on external landmarks for orientation. However, removing the visual cue did not immediately disrupt HD cell activity. Over time, though, the preferred firing direction gradually drifted, suggesting that internal self-motion cues also play a role in maintaining orientation but can accumulate errors. Additionally, changing the shape of the enclosure did not significantly alter the tuning properties of HD cells, reinforcing the idea that they primarily depend on visual landmarks rather than environmental geometry.

The stability of the HD cell signals depends on vestibular input, particularly from the dorsal tegmental nucleus (DTN) and lateral mammillary nucleus (LMN) [3, 4]. The DTN receives vestibular input and sends it to the LMN, which in turn projects to the anterior thalamus, where HD cells integrate this information. These structures help maintain the directionality of HD cells even when external landmarks are unavailable, providing a crucial internal reference. However, the loss of vestibular input can cause disorientation, leading to a drift in HD cell activity.

HD cells also interact with grid cells and place cells in the entorhinal cortex and hippocampus, contributing to spatial representation [2, 6]. While HD cells provide directional information, grid cells encode position using a periodic firing pattern, and place cells represent specific locations in the environment. This interaction supports spatial navigation by linking orientation and positional information. Notably, HD cells continue to fire coherently in darkness, primarily relying on self-motion cues, but their accuracy can degrade without periodic recalibration from visual landmarks or environmental boundaries [5].

B. Directional Tuning Curve

The typical tuning curve of an HD cell has a bell curve-like shape as shown in Figure 1A. The tuning curve is used to plot the firing rate (f) of the HD cell as a function of the difference between the head direction (θ) and the preferred head direction of the HD cell (θ_0). According to Zhang [1], the tuning curve of the HD cells in the postsubiculum and the anterior thalamus can be described analytically using a Gaussian-like function, which is related to the circular normal distribution function [7]. The tuning curve is given by the function:

$$f = A + B\mathrm{e}^{K\cos(\theta-\theta_0)} \tag{1}$$

Where A, B and K are the positive parameters that are selected so that the tuning curve fits the experimental data obtained by Taube [8] for both the postsubiculum and the anterior thalamus. While K determines the steepness of the tuning curve, A and $B\mathrm{e}^K$ determine the steady-state and the maximum firing rates respectively. From Figure 1, it is clear that the firing rate is the highest when the difference between the head direction (θ) and the preferred head direction of the HD cell (θ_0) is minimal.

III. BASIC MODEL

The HD system is modelled as a continuum network of neurons with a ring topology, in which each neuron corresponds to some preferred direction θ. The system dynamics are described by an integro-differential equation, which defines the time development of the synaptic input $u(\theta, t)$ from the contributions of all other neurons in the network. This formulation is necessary because HD cells do not function independently; rather, their activity is regulated by a broad array of synaptic interactions that establish their tuning properties. Unlike standard differential equations for local interactions, the integral term in Zhang's [1] equation accounts for the collective effect of all neurons on each other, enabling a more realistic description of HD network dynamics [1].

The governing equation for the model is:

$$\tau\frac{\partial u(\theta,t)}{\partial t} = -u(\theta,t) + [w * \sigma(u)](\theta,t) \tag{2}$$

$$[w * \sigma(u)](\theta,t) = \frac{1}{2\pi}\int_0^{2\pi} w(\theta-\phi)\sigma(u(\phi,t))\mathrm{d}\phi \tag{3}$$

Here $u(\theta, t)$ is the net synaptic input at time t, τ is the time constant (typically between 10 to 50ms), and $w(\theta-\phi)$ is the weight of synaptic connections between neurons sensitive to directions θ and ϕ. The function $\sigma(u)$ is a sigmoidal nonlinear activation function, which specifies the firing rate response as a function of the synaptic input. The tuning curve function (f) given by Equation (1) is reinterpreted as the average firing rate $\sigma(u)$ of all the HD cells with the same preferred direction θ. The integral is a convolution operation, summing the weighted inputs from all the neurons to compute the net input at each preferred direction.

It would be computationally expensive to calculate this convolution directly for every neuron, especially for many HD cells. To inexpensively

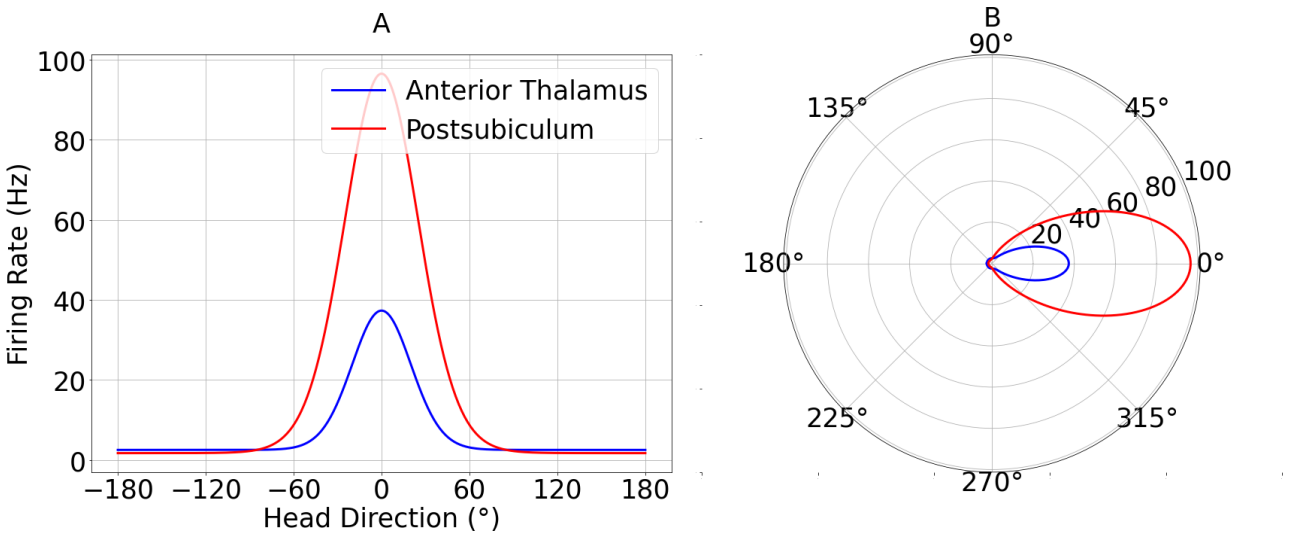

FIG. 1: **Tuning curve of a typical HD cell in both Polar and Cartesian coordinates.** Zhang [1] used the experimental data collected by Taube [8] to fit a Gaussian-like function (Equation (1)). We used this function to reproduce the tuning curves for the Anterior Thalamus and the Postsubiculum HD cells. The firing rate reaches its maximum value when the head direction (θ) and the preferred head direction of the HD cell (θ_0) are the same. For the anterior thalamus HD cell, which has a lower maximum firing compared to that of the postsubiculum cell, the parameter values used are $K = 8.08$, $A = 2.53$ Hz, and $Be^K = 34.8$ Hz. For the postsubiculum HD cell the parameter values used are $K = 5.29$, $A = 1.72$ Hz, and $Be^K = 94.8$ Hz.

compute this convolution, we used fast fourier transform (FFT) provided by the numpy package. By leveraging the convolution theorem, we can perform the computation in the frequency domain, where the convolution simplifies to an element-wise multiplication

$$F[w * \sigma(u)] = F[w] \cdot F[\sigma(u)] \tag{4}$$

where F denotes the Fourier transform. The inverse FFT (IFFT) is then used to transform the result back into the spatial domain. This approach significantly reduces the computational complexity from quadratic time $O(N^2)$ to logarithmic time $O(N \log_2 N)$ and enables real-time simulation of HD cell dynamics [9].

A key component of the model is the synaptic weight distribution function $w(\theta)$, which determines how neurons interact with each other based on the difference in their preferred directions. This function is decomposed into an even (symmetric) component w_{even} and an odd (asymmetric) component w_{odd}, expressed as:

$$w(\theta, t) = w_{\text{even}}(\theta, t) + w_{\text{odd}}(\theta, t) \tag{5}$$

The even component remains constant and defines the stable connectivity structure of the network, ensuring that HD cell activity forms a ring attractor—a self-sustaining pattern of activity centered around a single preferred direction. The odd component varies with time and introduces asymmetry into the system, allowing the activity bump to shift dynamically as the head moves. This mechanism is essential for updating the internal sense of direction based on movement.

Another critical aspect of the model is the tuning curve of HD neurons. The function $w_{\text{even}}(\theta)$ is designed to reflect the characteristic centre surround structure observed in HD networks, where neurons strongly excite nearby neurons with similar preferred directions while inhibiting neurons with dissimilar preferred directions. This ensures that HD cells exhibit a sharp, localized peak of activity that represents the current heading. The tuning curve is typically Gaussian-like, meaning neurons are most responsive to their preferred direction and gradually decrease activity as the angle deviates from the their preferred direction.

IV. STATIONARY SELF-SUSTAINING ACTIVITIES

Head direction (HD) cells have the capacity to maintain a stable representation of orientation even in the absence of external input. The specific arrangement of synaptic weight distribution and its interplay with the non-linear activation function gives rise to this self-sustaining activity. According to earlier research, these mechanisms enable HD networks to establish and maintain directional tuning, which enables a consistent and steady sense of orientation.

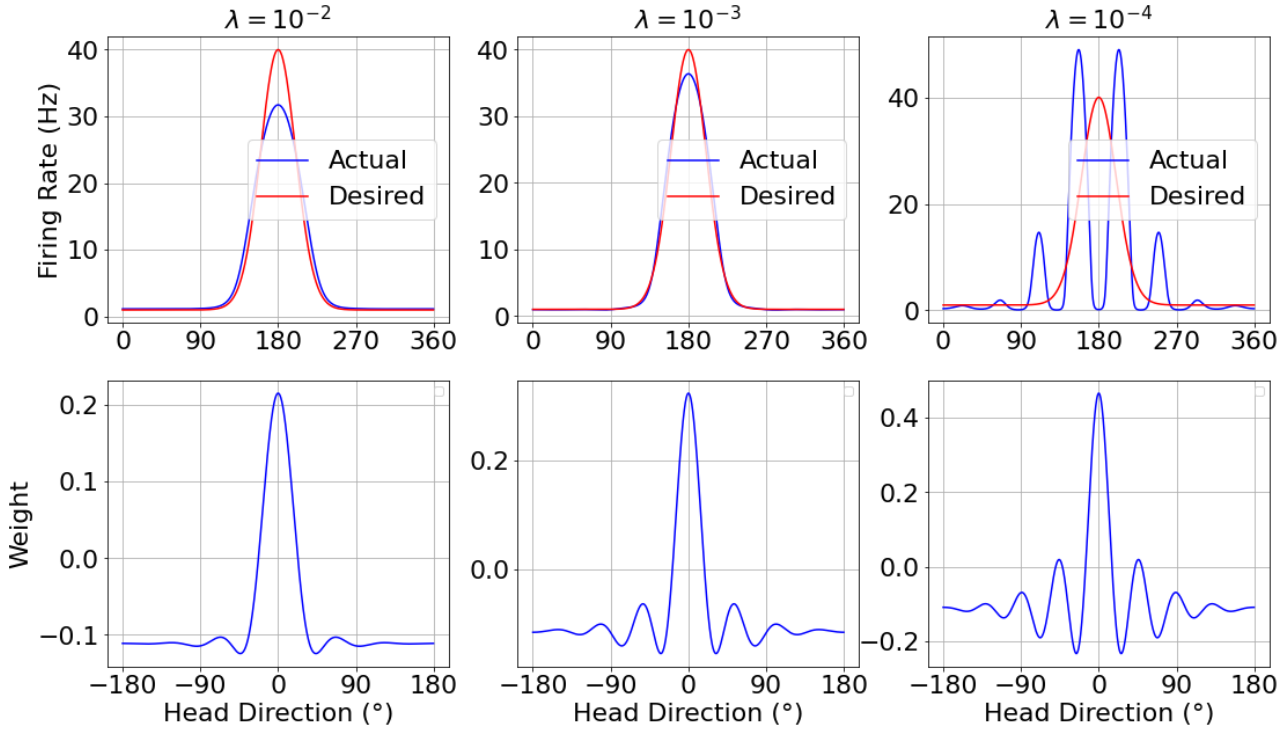

FIG. 2: **Synaptic weight distribution and regularisation.** The plot illustrates the effect of various strengths of weight regularisation. If regularisation is too strong, the stable firing profile becomes duller than the desired profile. If the regularisation is too weak, the stable profile will consist of several peaks. The predicted results for $\lambda = 10^{-3}$ align most closely with the desired profile.

A. Origin of Directional Tuning

Zhang [1] proposed a theoretical framework to explain the establishment of the HD cell network, emphasising the importance of symmetric synaptic connections. These connections exhibit both local stimulation and long-range inhibition, resulting in a network structure that spontaneously stabilises into a well-defined activity profile [1]. Computational modelling has demonstrated that, regardless of initial conditions, the network converges to a stereotyped pattern of activity. The system is rotationally invariant, which ensures that all the neurons follow the same interaction rules. However, the fully symmetric state, in which the neurons are either active or inactive, is unstable. Even small perturbations, such as inherent brain noise, can disrupt the symmetry and result in the formation of localised activity peaks. Skaggs et. al. [10] demonstrated that directional tuning emerges as a population-level property, where the collective activity of HD cells represents the head's orientation. Experimental studies by Taube [8] have also provided evidence that HD cell activity persists even in the absence of sensory input. Taube [8] recorded HD cell responses in total darkness and observed that their activity remained stable, suggesting that the network's internal dynamics are sufficient for maintaining orientation. Another key characteristic of the HD network is the rigid coupling of the preferred directions across different HD cells. Zhang [1] noted that once the network stabilises, the peak of the activity bump can be centred at any location in the ring attractor, reflecting a neutral equilibrium state. This property ensures that the system remains flexible while maintaining stability in directional representation.

B. Sigmoid Function

The model's stability is determined by the sigmoid function's shape, which in turn affects its attractor dynamics. The typical sigmoid function $(1 + e^{-x})^{-1}$ is symmetrical; yet this characteristic is not necessarily ideal for this model as the inherent symmetry of the typical sigmoid function limits the flexibility in modelling the nonlinear input-output relationship. By modifying the sigmoid function, the model can better approximate asymmetric dynamics that are perhaps more representative of the actual behaviour of the system. Thus, the model by Zhang [1] employs a non-standard sigmoid function shown in Figure 3. This non-standard sigmoid function is given by

$$\sigma(x) = a \ln^{\beta}(1 + e^{b(x+c)}) \tag{6}$$

For large $x > 0$, the function follows a power-

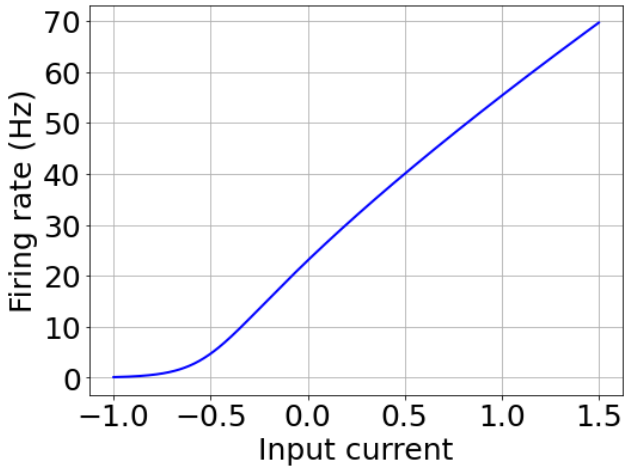

FIG. 3: **Sigmoid function.** The input current is represented in arbitrary units. The system exhibits a large firing rate at zero due to the presence of a constant bias c in the sigmoid function. The parameter values for β, b, c, and a are 0.8, 10, 0.5, and 6.34, respectively. The condition $\sigma(1-c) = f_{\max} = 40$ Hz is used to determine the parameters, ensuring the system operates within the desired firing range.

law behavior, scaling as x^{β}. For large $x < 0$, it decays logarithmically, flattening toward zero. Thus, in Equation 6, the positive half behaves as a power function with exponent β, while the negative half exhibits slower decay.

C. Synaptic Weight Distribution and Regularisation

The intricate neural network processes that are accountable for spatial orientation, particularly the head-direction (HD) cell network, rely heavily on synaptic weight distributions. The distributions of weight are important in establishing the activity patterns that enable animals and humans to preserve a sense of direction. At the basis of Zhang's [1] HD cell network model is the stationary state equation:

$$u = w * \sigma(u) \tag{7}$$

In Equation (7), u is the average net input to the HD cells, w is the synaptic weight distribution, and $\sigma(u)$ is the target firing profile. The equation represents the relationship between the input, the weights, and the output of the network. To further investigate the relationship, Zhang [1] applied Fourier analysis and thereby transformed the equation into the frequency domain:

$$\hat{u} = \widehat{\sigma(u)}\hat{w} \tag{8}$$

Where $\hat{u}$, $\hat{w}$, and $\widehat{\sigma(u)}$ are the Fourier coefficients of the respective functions. This transformation enables a more refined analysis of the behaviour of the network at various spatial frequencies. Theoretically, the weight distribution $\hat{w}$ would be derived by solving:

$$\hat{w} = \frac{\hat{u}}{\widehat{\sigma(u)}} \tag{9}$$

But this straightforward method has a serious problem. The Fourier components of $\hat{u}/\widehat{\sigma(u)}$ have a tendency to become very large at high frequencies, and the solutions diverge. This mathematical obstacle reflects the biological reality that neural networks cannot have infinitely fine spatial tuning. To handle this issue and enhance the biological plausibility of the model, Zhang [1] employed regularisation techniques. These techniques aim to balance the accuracy of the directional representation with the biological constraints of the synaptic weight distribution. This approach involves minimising an error function that is given by:

$$E = \frac{1}{2\pi}\int_0^{2\pi} \big(u(\theta) - (w * \sigma(u))(\theta)\big)^2 \mathrm{d}\theta + \frac{\lambda}{2\pi}\int_0^{2\pi} w^2(\theta)\mathrm{d}\theta \tag{10}$$

The parameter λ governs the balance between the accuracy and flatness of the solution. The final solution in the Fourier domain is :

$$\hat{w}_n = \frac{\hat{u}\widehat{\sigma(u)}}{\lambda + |\widehat{\sigma(u)}|^2} \tag{11}$$

The selection of the regularisation parameter λ is very important for the stability and performance of the network. Figure 2 illustrates the firing rate and weight distribution for various λ values. If λ is set too high, the weight distribution becomes too broad, and as a result, the directional tuning of HD cells loses accuracy. If λ is set too low, the weight distribution can become oscillatory, which can cause instability in the activity profile. Finding the right balance is important in order to create a model that not only captures directional orientation accurately but also maintains stability. As illustrated in Figure 2, $\lambda = 10^{-3}$ produces the closest firing rate and tuning curve to that of a typical HD cell shown in Figure 1. Therefore, for the remainder of this report, we used $\lambda = 10^{-3}$.

V. DYNAMIC SHIFT MECHANISMS

A. Basic Principles

The shift mechanism in head direction (HD) cells is essential for maintaining orientation representation as animals move their heads. This mechanism, as theorized by Zhang [1], operates through directionally biased reciprocal connections between HD cells, causing the activity profile to shift along the network in response to head movements. The mathematical formulation of this mechanism

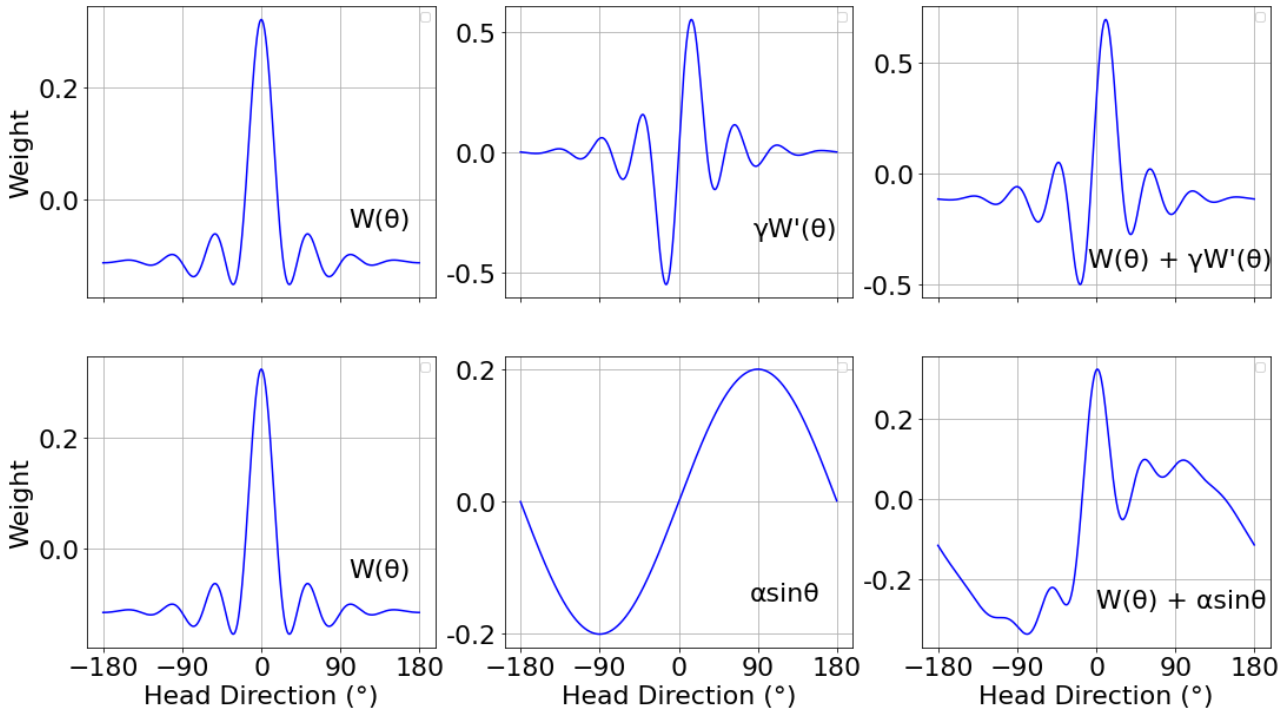

FIG. 4: **Weights modifications.** The plot shows the impact of the derivative-based and sinusoidal-based modifications on the weight distribution. γ and α are unitless constants set to -0.063 and 0.000201 respectively, these values were provided by Zhang [1].

involves modifying synaptic weights according to:

$$w(\theta, t) = W(\theta) + \gamma(t)W'(\theta) \tag{12}$$

where $W(\theta)$ represents the static weight distribution. We replicated this framework to test how different weight modification strategies affect the stability of the activity profile. Figure 4 shows the impact of the weight modifications on the weight distribution of the model. As shown in Figure 5, implementing an odd-weight component proportional to the derivative of the even-weight component resulted in smooth activity shifts without deformation, confirming Zhang's predictions [1]. In contrast, Figure 6 reveals that sinusoidal weight modification of the form

$$w(\theta, t) = W(\theta) + \alpha\sin(\theta) \tag{13}$$

causes severe profile distortions, with multiple peaks and discontinuities visible in both representations (Figure 6). This confirms Zhang's assertion that non-derivative odd components disrupt the stability of the shift mechanism [1]. The sinusoidal modification introduces periodic variation that does not align with the natural dynamics of the HD cell network, leading to instability and distortions in the activity profile. These findings align with Blair and Sharp's [11] biological observations that HD cell tuning curves remain stable during movement, suggesting biological HD networks likely employ derivative-based weight modifications to maintain a reliable orientation representation.

B. Spike Frequency Adaptation

We extended the original study by modelling the effect of spike frequency adaptation on the neural activity of the network. According to Benda et. al. [12], spike frequency adaptation refers to the process whereby a neuron decreases its firing rate over time in response to a steady input stimulus. This occurs due to inherent cellular mechanisms, such as the activation of slow ionic currents, which help neurons filter out prolonged, low-frequency stimuli, thereby enhancing their response to transient signals. In the context of the head direction cells, spike frequency adaptation is a convenient modelling option since it enables the system to modify and update its activity dynamically over time. In order to model spike frequency adaptation, we made the following changes to the model. Firstly, only the even component of the weights was used.

$$w(\theta, t) = W(\theta)$$

The model given in Equation (2) was modified as follows:

$$\tau_u \frac{\partial u}{\partial t} = -u - (g \cdot a) + w * \sigma(u) \tag{14}$$

$$\tau_a \frac{\partial a}{\partial t} = u - a \tag{15}$$

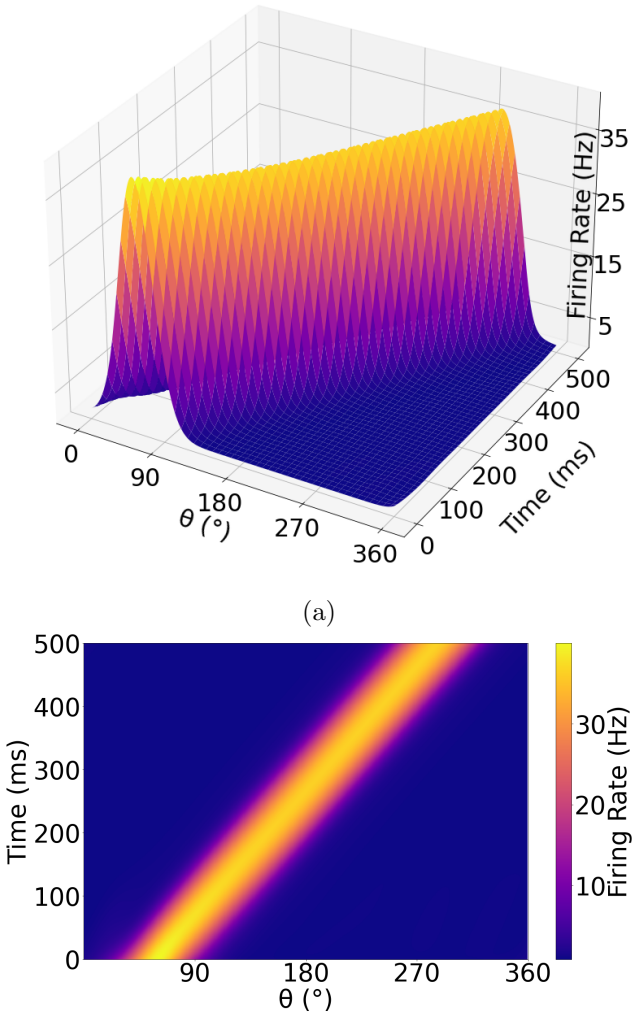

(a)

(b)

FIG. 5: **Weight modification with derivative.** The plot illustrates firing rate distribution using derivative-based odd-weight components. The plot additionally demonstrates a stable, smooth shift of the activity profile that maintains its shape over time. τ was set to 50ms.

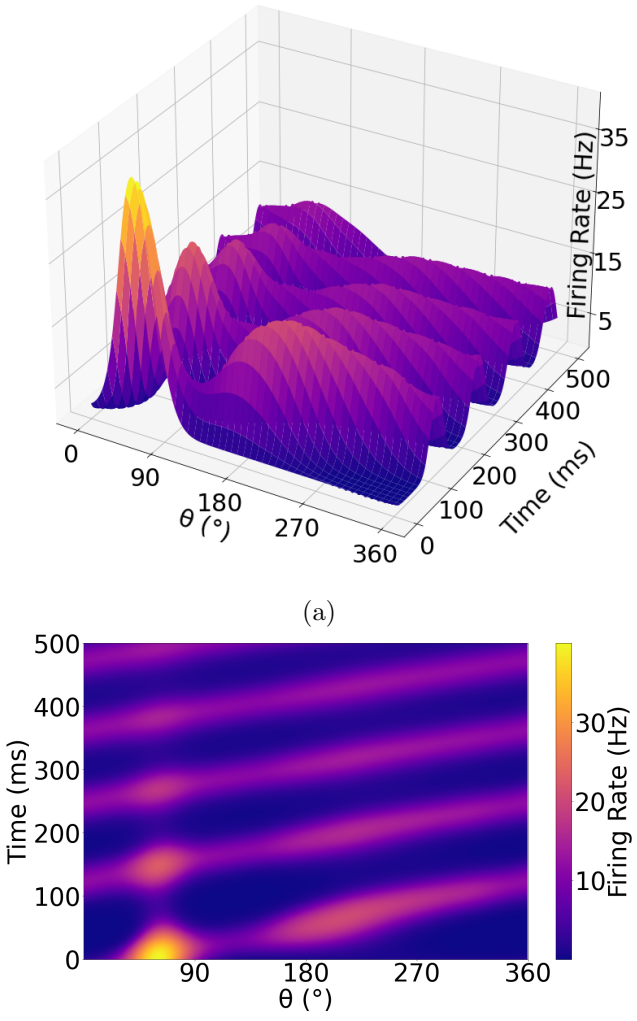

(a)

(b)

FIG. 6: **Weight modification with sine.** The plot shows firing rate distribution with sinusoidal odd-weight components. The plot additionally reveals that, unlike derivative-based modification, sinusoidal weights produce unstable shifts that distort the activity profile. τ was set to 50ms.

where g is a positive parameter which controls the effects of $a(\theta,t)$. We also chose values τ_a, such that it was substantially larger than τ_u. This was to ensure that the adaptation $a(\theta,t)$ evolved more slowly than $u(\theta,t)$.

Figure 7 illustrates how spike frequency adaptation induces oscillations and alters the time course of neural activity of the network. Initially, the system possesses a strong firing rate at a specific orientation. However, as adaptation kicks in, the peaks shift and successively decay, resulting in a drifting and weakening response over time. This effect is evident in the heatmap (Figure 7b), where the response bands gradually shift position and weaken, while the region of high activity oscillates. This result suggests that adaptation in head direction cells could play a role in slow drifts in perceived orientation, potentially impacting spatial navigation and memory.

C. Two Dimensional Analogy

The two-dimensional analogy by Zhang [1] is a generalisation of the head direction cell model to a continuous attractor network in more than one dimension. Here, the firing rate $f(\theta_x, \theta_y, t)$ and the net input $u(\theta_x, \theta_y, t)$ satisfy the relation $f = \sigma(u)$, as in the one-dimensional model. The input to the system is described by the convolution below:

$$[w * \sigma(u)](\theta_x, \theta_y, t) = \int_{-\infty}^{\infty}\int_{-\infty}^{\infty} w(\theta_x - \theta'_x, \theta_y - \theta'_y, t)\sigma(u(\theta'_x, \theta'_y, t))\mathrm{d}\theta'_x\mathrm{d}\theta'_y \tag{16}$$

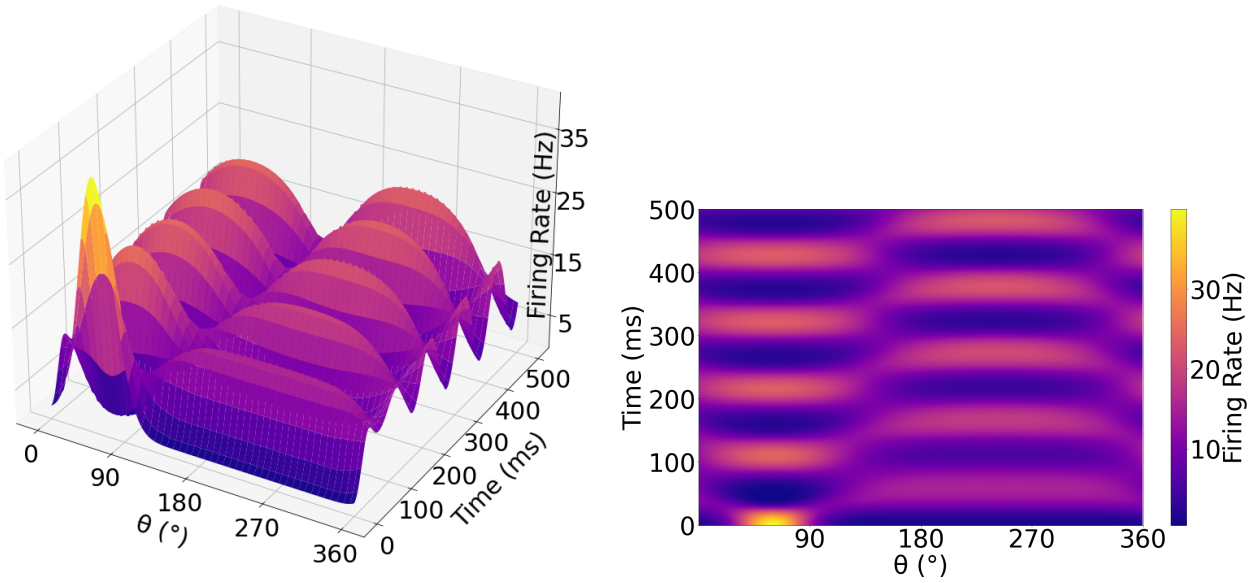

(a) (b)

FIG. 7: **Effect of Adaptation on the Temporal Dynamics of Head Direction Cell Activity.** The impact of adaptation on the firing rate of a head direction cell network. (a) A 3D surface plot of firing rate as a function of head direction angle θ and time. (b) A heatmap of the same plot, with colour intensity indicating firing rate as a function of time. Adaptation causes the gradual shift and reduction of the peak firing rates over time. The parameters values for g, τ_a and τ_u are 2, 50 ms and 10 ms respectively.

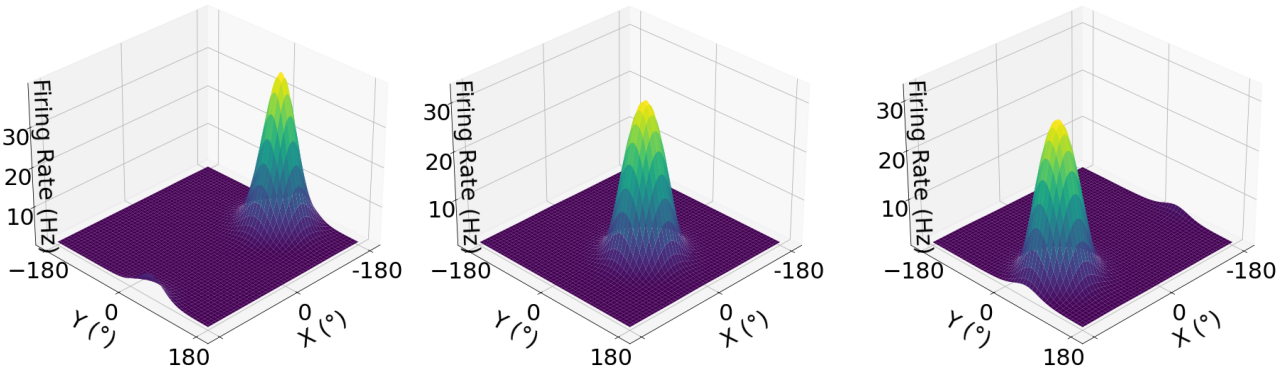

(a) time = 0ms (b) time = 300ms (c) time = 500ms

FIG. 8: **Two dimensional network.** Simulation of a two-dimensional head direction cell network, illustrating the propagation of the activity bump in a stable fashion. The model accurately replicates the findings of Zhang [1], whereby local activity propagates unchanged. Unlike Zhang [1], the position is plotted in angular coordinates rather than centimetres. τ was set to 50ms.

where the weight distribution function $w(\theta_x, \theta_y, t)$ allows a stable localised activity bump to propagate undistorted. We were successfully able to replicate these findings in our simulation, as shown in Figure 8, where the moving bump continues to remain stable as it propagates over time. The slight deviation from the paper is that whereas the position in the figures in Zhang [1] were given in centimetres, our figure shows it in angular coordinates. Regardless of this, the basic dynamics are unchanged, confirming the findings of Zhang [1].

VI. DELAYED DIFFERENTIAL EQUATION

A. Basic Principles

In the original paper, Zhang [1] modelled the ongoing attractor dynamics of head-direction (HD) cells with an integro-differential equation and successfully described their function in representing head orientation. A key limitation of the model

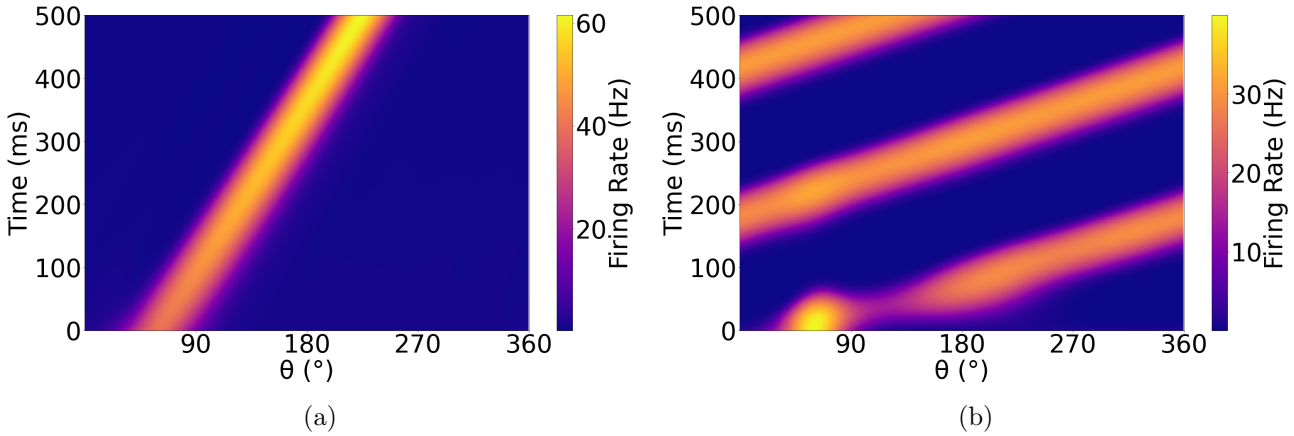

(a) (b)

FIG. 9: **Heatmaps of the firing rate in the DDE model.** (a) The DDE model with a derivative-based odd-weight component shows a smoothly propagating bump, although the bump has a higher firing rate compared to that of the original model. (b) The DDE model with a sinusoidal odd-weight component shows a pronounced oscillatory pattern with discrete bands of high activity instead of a continuous drift with a low firing rate. τ_u and τ_α were set to 50ms and 10ms respectively.

was that it presumes instant neuronal interactions and disregards the finite processing and transmission times that are a hallmark of neural systems.

To address this limitation, we further extended the model by including delay differential equations (DDEs) that explicitly include time delays in the transmission of neuronal signals and synapse processing. This allowed for more realistic modelling of the timing dynamics of HD cells, including anticipatory firing and head movement signal integration dependent on time, and enhanced the biological accuracy and predictive capability of the model [13]. The Python ddeint package was used to solve the DDE model given below.

$$\tau_u \frac{\partial u}{\partial t} = -u + [w * \sigma(u_{\tau_\alpha})] \quad \text{where} \quad u_{\tau_\alpha} = u(\theta, t - \tau_\alpha) \tag{17}$$

B. Firing Rate and Bump Dynamics

The incorporation of delays into the DDE model profoundly changes the dynamics of the head direction cell network. Comparing Figure 5 and Figure 9a, the derivative-based odd-weight configurations given by Equation (12) generate a stable, propagating activity bump in both the original and DDE models. The bump produced by the DDE model, as illustrated in Figure 9a, exhibits a higher firing rate as it propagates through the plane, though its speed of propagation is slower than that of the original model. In contrast, Figure 6 vs. Figure 9b, sinusoidal-based weight settings given by Equation (13) have oscillatory impacts on both models. However, in the DDE model illustrated in Figure 9b, the oscillations are much more pronounced, producing discrete phase shifts with higher firing rates, as opposed to the smoother trajectory of the original model shown in Figure 6. This reinforces the idea that delays inserted into periodic activity patterns sharpen them, which is supportive of the stabilising and organising role of delayed feedback in head direction cell activity.

We directly compared the dynamics of the original model and the DDE model in various regimes. Figure 10a shows the peak firing rate of a stationary bump plotted as a function of time, where both models undergo a slow decrease in their firing rate, with the DDE model always having a higher firing rate compared to the original model. Figure 10b shows the peak firing rate of the travelling bump and demonstrates a clear distinction between models—while the original model settles to a lower firing rate, the DDE model keeps growing, showing that delays facilitate activity propagation. Lastly, Figure 10c shows the angle of maximum firing rate of the travelling bump, illustrating that the bump in the DDE model propagates at a slower speed than in the original model. These results indicate that incorporating delays into the model introduces more complex temporal dynamics, leading to slower yet more sustained activity propagation. This can be crucial for accurately modelling biological systems where transmission delays influence network dynamics.

C. Speed of Propagating Bumps

Further, we examined how the speed of the propagating bumps in the head direction cell network is influenced by the γ parameter. At discrete time steps separated by τ_u, the function $\theta_{\max}(t)$ finds the location of the firing rate. We chose a very small time step τ_u such that, over the computed

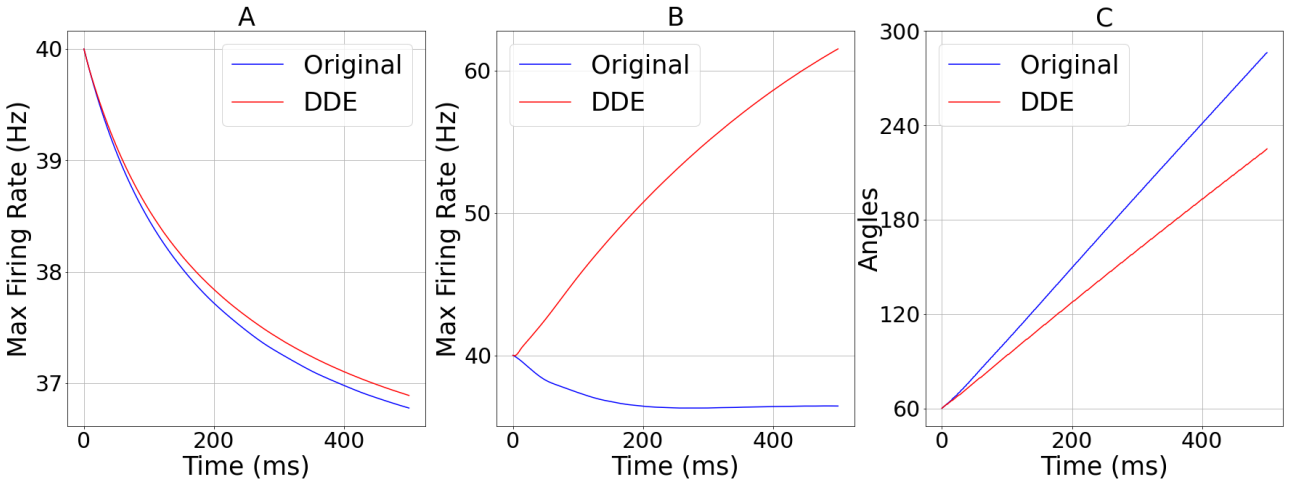

FIG. 10: **Comparison of Firing Rate and Bump Dynamics in the Original and DDE Models.** (A) Maximal firing rate of a stationary bump, in which the DDE model maintains a slightly higher rate. (B) Maximal firing rate of a travelling bump, where the DDE model continues to grow. (C) The direction of the maximal firing rate of the travelling bump, where the DDE model propagates more slowly.

time period, less than one full rotation across the entire range of angles was completed. For our speed computation, we considered only the time-frame from 100 to 300 milliseconds, returning the average of four speed measurements. Note: computing the speed over the entire simulation time-frame with a different τ_u value still returned the same value.

$$\theta_{\max}(t) = \arg\max_{\theta} \sigma(u(\theta, t)) \tag{18}$$

The angular speed is first computed using the equation below. The speed in radians per millisecond is then converted to degrees per second.

$$\omega(t) = \frac{180}{\pi} \cdot \frac{|\theta_{\max}(t+\tau_u) - \theta_{\max}(t)|}{\tau_u/1000} \tag{19}$$

Finally, the function returns the mean absolute speed over the time window:

$$\bar{\omega} = \frac{1}{4} \sum_{\substack{t=100 \\ t=t+\tau_u}}^{250} |\omega(t)| \tag{20}$$

As shown in Figure 11, both models exhibit a tendency of reducing speed as γ approaches zero. However, the DDE model consistently forecasts slower speeds than the original model across all γ values. This is indicative of the fact that the inclusion of delays in networks reduces the spread of activity, most probably as a result of temporal dependencies caused by delayed feedback.

D. Power Spectral Density (PSD)

Power spectral density (PSD) analysis is one of the basic methods in neuroscience used to describe the

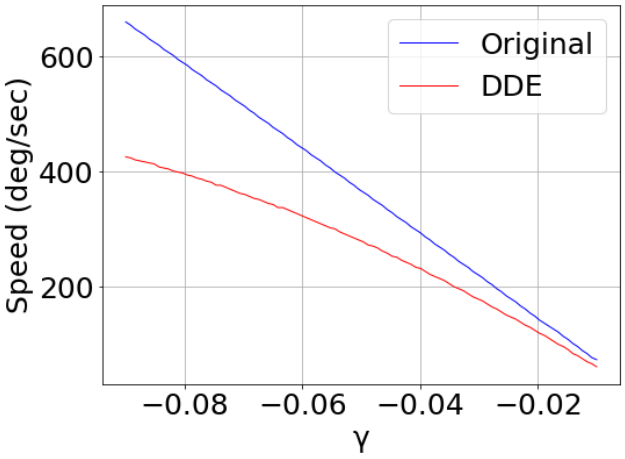

FIG. 11: **Effect of γ on the Speed of Travelling Bumps in the original and DDE Models.** The speed decreases as γ approaches zero, with the DDE model consistently exhibiting lower speeds than the original model, showing how the dynamics of bump propagation is influenced by time delays.

frequency contents of neural signals. PSD analysis reveals the distribution of power across different frequency bands and can be used to identify and measure oscillatory activity in neural systems. PSD analysis is critical to the comprehension of the internal neural processes since individual frequency components are usually linked with specific cognitive processes and behavioural states [14, 15].

In the context of head direction (HD) cells, PSD analysis enables us to examine how neuronal activity patterns change over time and whether the network dynamics are stable, oscillatory, or noisy. Because the introduction of delays in the

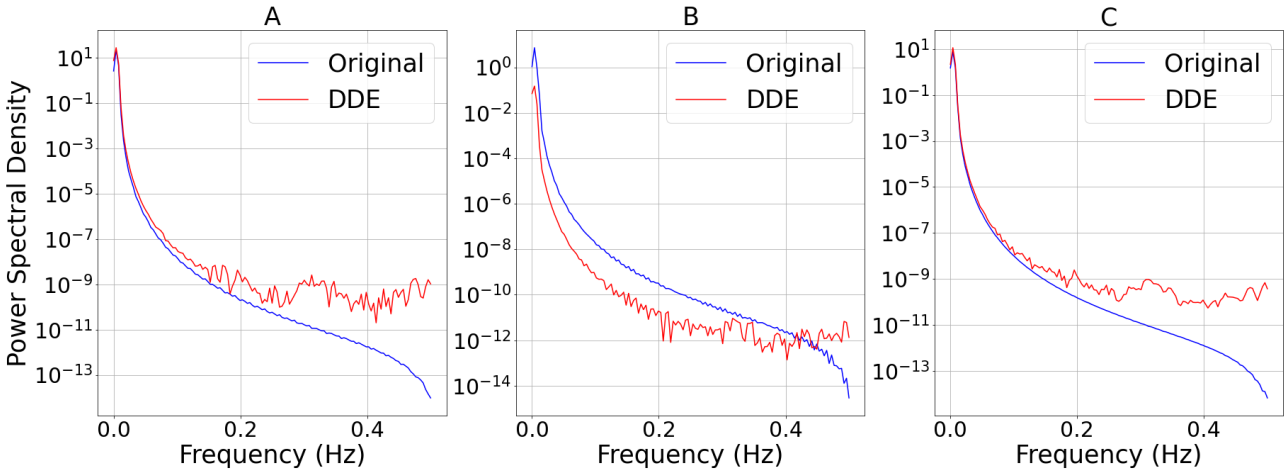

FIG. 12: **Comparison of PSD Between the ODE and DDE Models of Head Direction Cells.** The PSD of the ODE and the DDE at various head direction angles, (A) PSD at 158°, (B) PSD at 228°, and (C) average PSD over all angles. Delays introduced in the DDE model create power at lower frequencies, suggesting more complex temporal dynamics than in the original model.

DDE model changes the time structure of the network, a comparison of the PSD of the original and DDE models inform us about the implications of introducing such delays in the stability and rhythmicity of HD cell activity.

When the PSD of the original model is compared to that of the DDE model, clear differences are apparent. Figure 12a, plotting the PSD at 158 degrees, shows that the DDE model has extra spectral peaks at lower frequencies compared to the original model. This indicates that the inclusion of delays add slower oscillatory components, which may capture more intricate temporal dynamics. Figure 12b, at 228 degrees, confirms the observation, with the DDE model also having a wider range of power over frequencies, suggesting a more abundant frequency spectrum. Figure 12c, averaging the PSD over all angles, suggests that the DDE model has more power at lower frequency bands consistently compared to the original model. These results show that incorporating delays into the model more accurately captures temporal dependencies and feedback loops, providing a clearer representation of the system's dynamics.

VII. DISCUSSION

A. Computational Modeling of Head Direction Cells and Human Perception

Computational models of head direction (HD) cells explain how humans maintain orientation by integrating vestibular, proprioceptive, and visual inputs. Attractor network models simulate stable HD activity, allowing for persistent directional coding even in the absence of landmarks [10]. These models support path integration, a process in which self-motion cues update spatial position and facilitate navigation [16]. However, in the absence of external cues, HD signals gradually drift due to accumulated error. Such models also provide insights into human spatial perception, illustrating how the brain constructs and maintains an internal sense of direction.

B. Relation to Artificial Intelligence(AI)

Numerous researchers have explored the feasibility of using networks inspired by the head direction cell for navigation tasks [17–20]. Bing and his colleagues [17] recognised the promise of biologically inspired models for improving artificial navigation systems. By applying principles of head direction cells, the proposed head direction Cell (HDC) model is a biologically plausible and computationally efficient solution for real-world robot applications [17]. The HDC model relies on a continuous attractor network (CAN) with angular velocity inputs to ensure an accurate representation of the heading direction [17]. The model has three major components: the HDC layer, which encodes the heading direction; shift layers, for updating the direction continuously; and turning cells, to accumulate the angular velocity inputs [17]. The model functions well with minimal sensory input, which makes it resilient in situations where the surrounding landmarks may be deemed unreliable [17].

The benefits of this HDC model are high accuracy, real-time performance on low-power hardware, and biological plausibility. It is nevertheless not devoid of limitations, such as susceptibility to noisy input, lack of landmark-based corrections, and high computational cost in large-scale applications.

The model has been validated by both simula-

tion and experimental results using real robots, confirming the model's accuracy and usefulness [17]. This model can be further extended to autonomous cars, search-and-rescue robots, and neuroscience experiments. Future work can include the combination of HDCs with grid and place cells, thus taking cognitive navigation systems a step further and closing the gap between artificial intelligence and neuroscience.

VIII. CONCLUSION

We successfully replicated the findings of Zhang [1] on the intrinsic dynamics of head direction cell ensembles and expanded the model by adding delay differential equations. With the addition of delays, we found more complex temporal dynamics, such as slower propagation of activity and larger oscillatory dynamics. These results emphasise the significance of time dependencies in neural networks and demonstrate that incorporating biologically realistic delays can enhance our knowledge of spatial orientation and navigation.

[1] Kechen Zhang, "Representation of spatial orientation by the intrinsic dynamics of the head-direction cell ensemble: a theory," Journal of Neuroscience **16**, 2112–2126 (1996).

[2] Robert U. Muller, James B. Ranck, and Jeffrey S. Taube, "Head direction cells: properties and functional significance," Current Opinion in Neurobiology **6**, 196–206 (1996).

[3] Jeffrey S. Taube, "Head direction cells and the neurophysiological basis for a sense of direction," Progress in Neurobiology **55**, 225–256 (1998).

[4] Benjamin J. Clark and Jeffrey S. Taube, "Vestibular and attractor network basis of the head direction cell signal in subcortical circuits," Frontiers in Neural Circuits **6** (2012).

[5] Jeffery S. Taube, Robert U. Muller, and James B. Ranck, "Head-direction cells recorded from the postsubiculum in freely moving rats. ii. effects of environmental manipulations," Journal of Neuroscience **10**, 436–447 (1990).

[6] Torkel Hafting, Marianne Fyhn, Sturla Molden, May-Britt Moser, and Edvard I. Moser, English"Microstructure of a spatial map in the entorhinal cortex," Nature **436**, 801–6 (2005).

[7] Norman L. Johnson, Samuel Kotz, and Narayanaswamy Balakrishnan, *Continuous univariate distributions, volume 2* (John wiley & sons, 1995).

[8] Jeffrey S. Taube, "Head direction cells recorded in the anterior thalamic nuclei of freely moving rats," Journal of Neuroscience **15**, 70–86 (1995).

[9] James W. Cooley and John W. Tukey, "An algorithm for the machine calculation of complex fourier series," Mathematics of computation **19**, 297–301 (1965).

[10] William E. Skaggs, James J. Knierim, Hemant S. Kudrimoti, and Bruce L. McNaughton, "A model of the neural basis of the rat's sense of direction," in *Advances in Neural Information Processing Systems*, Vol. 7 (1995) pp. 173–180.

[11] Hugh T. Blair and Patricia E Sharp, "Anticipatory head direction signals in anterior thalamus: evidence for a thalamocortical circuit that integrates angular head motion to compute head direction," J. Neurosci. **15**, 6260–6270 (1995).

[12] Jan Benda, André Longtin, and Len Maler, "Spike-frequency adaptation separates transient communication signals from background oscillations," Journal of Neuroscience **25**, 2312–2321 (2005).

[13] Alex Roxin and Ernest Montbrió, "How effective delays shape oscillatory dynamics in neuronal networks," Physica D: Nonlinear Phenomena **240**, 323–345 (2011).

[14] Sadi Md Redwan, Md Palash Uddin, Anwaar Ulhaq, Muhammad Imran Sharif, and Govind Krishnamoorthy, "Power spectral density-based resting-state eeg classification of first-episode psychosis," Scientific Reports **14**, 15154 (2024).

[15] Srishty Aggarwal and Supratim Ray, "Slope of the power spectral density flattens at low frequencies with healthy aging but also steepens at higher frequency in human electroencephalogram," Cerebral Cortex Communications **4**, tgad011 (2023).

[16] Bruce L. McNaughton, Francesco P. Battaglia, Ole Jensen, Edvard I. Moser, and May-Britt Moser, "Path integration and the neural basis of the cognitive map," Nature Reviews Neuroscience **7**, 663–678 (2006).

[17] Zhenshan Bing, Amir EI Sewisy, Genghang Zhuang, Florian Walter, Fabrice O Morin, Kai Huang, and Alois Knoll, "Toward cognitive navigation: Design and implementation of a biologically inspired head direction cell network," IEEE Transactions on Neural Networks and Learning Systems **33**, 2147–2158 (2021).

[18] Raphaela Kreiser, Matteo Cartiglia, Julien NP Martel, Jörg Conradt, and Yulia Sandamirskaya, "A neuromorphic approach to path integration: a head-direction spiking neural network with vision-driven reset," in *2018 IEEE international symposium on circuits and systems (ISCAS)* (IEEE, 2018) pp. 1–5.

[19] Zhenshan Bing, Dominik Nitschke, Genghang Zhuang, Kai Huang, and Alois Knoll, "Towards cognitive navigation: A biologically inspired calibration mechanism for the head direction cell network," Journal of Automation and Intelligence **2**, 31–41 (2023).

[20] Thomas Degris, Loıc Lacheze, Christian Boucheny, and Angelo Arleo, "A spiking neuron model of head-direction cells for robot orientation," in *Proceedings of the eighth int. conf. on the simulation of adaptive behavior, from animals to animats* (2004) pp. 255–263.